KMS Technologies – KJT Enterprises Inc.

Chapter 8
Case Histories :
Resolving Resistive Layers with LOTEM

extract from

Strack, K.-M., 1992, reprinted 1999
Exploration with deep transient electromagnetic: Elsevier, 373 pp.

KMS Technologies – KJT Enterprises Inc.
6420 Richmond Ave., Suite 610
Houston, Texas, 77057, USA
Tel: 713.532.8144

Please visit us
http://www.kmstechnologies.com

Chapter 8
Case Histories:
Resolving Resistive Layers
with LOTEM

One of the most difficult tasks for electromagnetic geophysicists is the development of new applications of EM techniques. In the exploration environment the physics of EM methods are often either not clearly understood or the capabilities are incompletely evaluated. Some of the newer applications of the LOTEM technique are demonstrated in this chapter. Although mostly simple one- or two-channel field systems have been used to date, the results show a very promising potential for newer applications. The first two case histories cover the resolution of resistive layers using the LOTEM technique. The information presented here is based on a paper by Strack et al (1989). The first successful field tests of applying LOTEM with electric field measurements were pioneered by Vozoff in Australia and subsequently the work was continued in FRG. Following, a case history from China is shown, where the use of the technique was demonstrated to a structure involving carbonates.

In areas of basalt cover, crystalline overthrusting or surface carbonates (Berkman et al, 1983; Andrieux and Wightman, 1984, Prieto et al, 1985; Stanley et al, 1985) electromagnetic methods have been successful, because they respond to different physical properties than seismics. However, since electromagnetic methods do not have the intrinsic resolution of reflection seismics, it is very important to utilize the available resolution of EM to the fullest. The next step, beyond passive EM methods such as magnetotellurics (MT), is the use of a controlled source method such as transient EM which might offer higher resolution.

Here the case histories follow the work of Eadie (1981) and Verma and Mallick (1979). The first is an exploration problem from an oil field in Europe where a resistive layer had to be defined in an oil-producing environment. In the second case history, LOTEM was applied in Australia to define porous regions in a carbonate within a sedimentary sequence. In both cases interpretation was assisted by inversion using models incorporating prior information such as well logs, reflection seismics and/or geology.

EXTENSION OF THE PHYSICAL CONCEPT TO
RESISTIVE LAYERS

In chapter 2, the basic physical background of the LOTEM method were discussed and the smoke ring concept was introduced. Now, let us compare the effect of conductive and resistive layers embedded in a medium resistive host. To visualize the current flow in the subsurface, figure A.7.6 (appendix 7, color figures) shows contours of current densities for a conductive (left, 1 Ωm) and a resistive (right, 400 Ωm) layer in a half-space of intermediate resistivity (20 Ωm). The individual frames are snapshots in time starting with 0.01 seconds at the top to 1 second for the bottom frames. The difference between the left and right sides lies in the current densities within the second layer. For the conductive case (left column) the currents remain relatively longer within the conductive layer. For the resistive case there are no induction currents visible in the resistive layer. A secondary contribution to the electric fields is due to a charge accumulation at the horizontal interfaces for the resistive layer resulting from vertical current flow. In the conductive layer case most of the energy is transmitted through the second layer by currents. For the resistive case the magnetic field carries the currents through the layer.

All inductive electromagnetic sources – such as used with MT and large loop EM methods – can only induce horizontal induction current flow in the subsurface (Verma and Mallick, 1979; Boerner, 1992). The galvanic part of the grounded electrical dipole causes a vertical component of the electric field (Nekut and Spies, 1989). This component generates electrical charges at the horizontal layer boundaries. The frames in figure A.7.7 are horizontal sections at the top of the second layer for different times. They can be pictured as a horizontal time slices through a vertical smoke ring. These time slices show the distribution of the charge density for the resistive (right column) and for the conductive (left column) case of figure A.7.6. The charges are positive (yellow and red colours) when the electric field points from a conductor towards a resistor. They are negative (green and blue colours) when the electric field points towards a conductor. The polarity of these charges depends on a) the transmitter polarity and b) the jump in the electric field which is needed in order to satisfy the continuity of the normal current density component. The charges have opposite signs on either side of the transmitter. They also have opposite signs according to whether the bed is resistive or conductive (compare left with right column). The latter means that the charges are sensitive to the resistivity contrast at the layer boundary. Any measurable effect of the charge accumulation should therefore be a good indicator of the embedded layer resistivity. Initially, the lateral moveout in both cases is the same. Then the charge build–up moves out faster for the resistive case. The bottom two frames show that the uniformity of the charge distribution increases with time, but proceeds faster in the resistive case. The charge distribution on the resistive layer is also stronger for all times. However, the electric charges at the second layer remain longer at the interface for the resistive case. As a

result, conductive targets can be found measuring the effect of the induction currents (figure A.7.6) and resistive targets by measuring the effect of the charges at the resistive layer interface (figure A.7.7). In both cases, when the conductive or resistive layer becomes too thick or its resistivity too extreme, it will act as a screening layer masking the section below.

One can simplify the explanation by describing the measurements of electric and magnetic fields as a combination of time focussing electromagnetic soundings with DC–resistivity soundings. This means through the grounded dipole transmitter and the electric field sensors one carries out a dipole–dipole sounding with the time and the volume focussing effect of the temporal diffusion of the induction current. In this one has more depth resolution (due to smaller volumes of integration) because of the transient phenomenon.

The two test surveys were done with different sets of hardware. In Europe we used DEMS IV (Digital Electromagnetic System, IVth generation) – the system described in chapter 5. In Australia a Zonge GDP 12 receiver (with a special LOTEM preamplifier) and transmitter (25 kVA), especially modified for the survey, were used. In both systems the magnetometers consisted of large multiturn loops with effective areas of the order of 200 000 squaremeters laid flat on the surface. Transmitter dipoles were wires 1–1.5 km long, earthed at each end. The electric fields were measured between grounded copper–copper sulphate non–polarizing electrodes 100 m apart. In both systems, the transmitter injected commutated currents with periods of seconds to minutes.

In the Zonge equipment, a current of 30 Amperes was maintained, and both E and H signals were recorded (with or without stacking) in the two–channel receiver. The incoming signal traces could be observed in real time on a portable oscilloscope. The DEMS IV receiver also allows online quality control and storage of individual transients. The DEMS IV transmitter injects currents of the order of a hundred Amperes provided by a high power switch/rectifier which uses all three phases of an 80 kVA motor generator. Transmitter switching and receiver sampling in both systems were synchronized by precision quartz oscillator clocks. Preamplifiers/filters located near the sensor units sent signals in the millivolt–to–volt range to the main amplifier/filter units and from there to the digital data acquisition systems.

EUROPEAN CASE HISTORY

A test survey was carried out in Europe with the objective of mapping geologic structure in an area of known geology over an oil field. In this, as in many other areas, the zone of interest was electrically resistive. On the basis of earlier suggestions by Eadie (1981), verified in Australia, electric field measurements were used in addition to the magnetic fields for better resolution of resistive features.

Figure 8.1 shows a survey plan of the test profile over an oil field. The sites shown on the map are only a small part of a larger survey. The receiver locations were

occupied twice, from two different transmitters, one located in the northeast and in the southwest, respectively. This was done primarily to see whether structural complications might lead to different interpretations for the data from the different transmitters. Currents of 50 and 150 Amperes were used at the different transmitters. Both transmitters gave comparable results as indicated by the two inversion results at station –2 shown in figure 8.2. The slight differences can be attributed to the smaller signal–to–noise ratios and the shorter recording time (higher sampling rate) for transmitter A measurements. Thus, for this survey we assumed the validity of one–dimensional inversion.
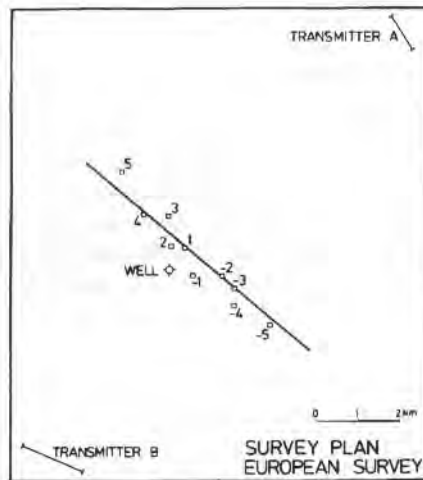

Fig. 8.1: Transmitter and receiver survey plan (partial) of the European test. Station numbers start with 0 at the well, going positive in the western and negative in the eastern direction (after Strack et al, 1989b).

Since the survey area is over an oil–producing field some pipelines and wells existed. In order to evaluate whether these distort the signal by either induced polarization or current channeling near the transmitter, routine walkaway tests are done (receiver locations not shown here). This means that the receiver is moved along the equator of the transmitter. Because for the LOTEM system used for this survey the system response was about 100 ms long, early time pipeline effects would be attenuated. Only if they are very strong they would show as reversals on the walkaway test (compare chapter 4). For this survey area the walkaway test did not show any anomalous behavior which is mainly because pipeline response in this area lies in a frequency range which is filtered out by the analog filters (which are required due to the strong cultural noise). Furthermore, the receivers were kept at least 50 meters away from the pipelines and 200 meters from pumping wells in order to avoid excessive electromagnetic noise in the measurements.
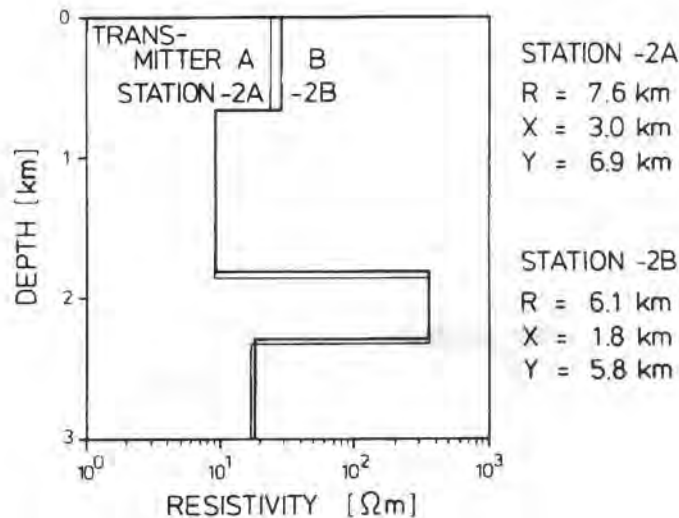
Fig. 8.2:   Comparison of inversion results at station −2 for two different transmitter locations displayed on a log–linear scale (after Strack et al, 1989b).

Examples of the magnetic and electric field transients and their respective processing steps for station 4 on this profile are shown on figure 8.3. The upper two frames show a raw transient for the magnetic (left) and the electric field (right). Below, their amplitude spectra are displayed. These spectra are used only for quality control and to define accurately the noise frequencies for each individual transient. These noise frequencies are then removed using recursive filters which retain true amplitudes (third pair of frames). Finally, the individual transients (routinely 50) are selectively stacked, rejecting the sporadic noise (Strack et al, 1989). The resulting stacked transients are shown at the bottom. After this processing the raw voltages are converted to true magnetic and electric fields. The magnetic fields are then corrected for first order transmitter overprint (Zonge et al, 1986) using the calibration factor described in chapter 3. The data are then converted to the logarithmic domain and resampled for data reduction. The reduced data are input into the inversion routines (Strack, 1984). At this stage we use a parametric inversion described by Jupp and Vozoff (1975), Vozoff and Jupp (1975) and Raiche et al (1985), which also outputs error statistics and a detailed resolution analysis of the individual model parameters. Some of the transients (less than 10%) were too strongly distorted by cultural noise to be interpreted.

For the starting model required for the inversion was derived from the well log. This was reduced to a sequence of models having various numbers of layers in order to obtain the simplest model which would explain the observed transients. The inversion outputs for the useable magnetic fields at each receiver position are shown in figure 8.4. The statistics output of the inversion program contains three different

pieces of information which show the model resolution (Raiche et al, 1985) (compare also chapter 4 and appendix 3):

○ The normalized singular values of the Jacobian (sensitivity) matrix indicate the *confidence* in each eigenparameter.

○ The transformation matrix from the eigenparameter domain to the physical parameter domain indicates which *combination* of layer resistivities, layer thicknesses, and depths–to–base are represented by each eigenvector.
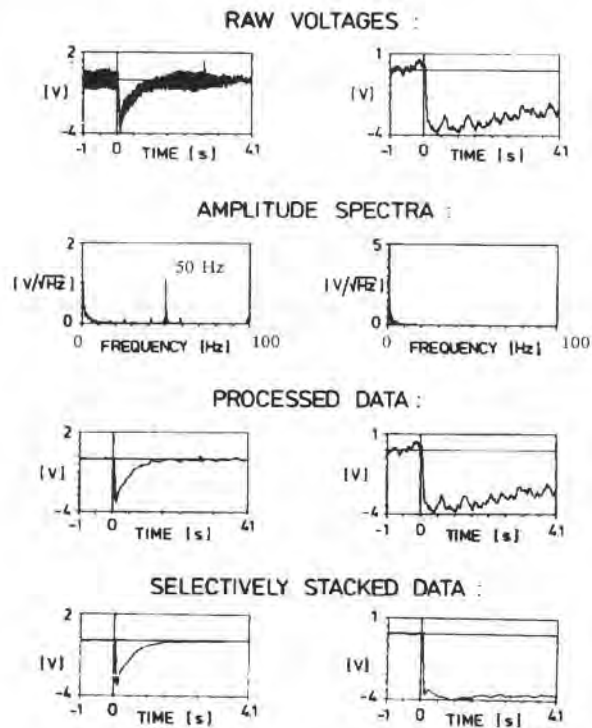

Fig. 8.3: Intermediate results from the data processing at one station of the test profile in figure 8.1. The magnetic response (time derivative of the magnetic field) is shown on the left column and the electric field signal on the right (after Strack et al, 1989b).

○ The damping factors for the original parameters are measures of the *importance* of each resistivity, thickness or depth–to–base in the fit of the calculated curve. Resistivities of the upper two layers and their respective thicknesses were well resolved. Their importance are above 80% and they are contained in the eigenvectors with confidences above 70%. The resistivity of the resistive layer (hatched) was poorly resolved. Its importance was below 1%, and it was not contained in the eigenvector with the highest confidence.

Figure 8.5 shows a profile with the usable electric field inversion results. The electric field resolves the layer parameters (resistivities and thicknesses) of the top two layers, but not quite as well as the magnetic field (importances between 50% and 80%). However, both the thickness of the resistive third layer, and its resistivity were better resolved by the electric field data with importances between 10% and 30% as compared to less than 1% for the magnetic field data. The consistency in the third layer of the magnetic field inversions across the profile is only because the third layer is input as starting model.

This difference in sensitivity to the resistive layer parameters was analyzed with the Jacobian matrix. The blocked resistivity log served as a representative model for the survey area to generate synthetic electric and magnetic field data. The Jacobian was then calculated by inverting both synthetic data sets with the well log as starting model. Each column of this matrix is a measure of the sensitivity of the data set to variations in the corresponding earth parameter. Figure 8.6 shows the sensitivities to variations of the parameters of the intermediate (resistive) layer and has little sensitivity to thickness changes of this unit. The magnetic field appears almost insensitive to changes in the resistivity of the resistive layer whereas the electric field shows strong effects for both resistivity and thickness variations.

The above results show that LOTEM measurements can be made successfully in the electrically noisy environment of industrialized Western Europe. The resistive layer parameters could be resolved over a producing oil field. The initial objective of the survey to match the well log was successfully achieved. Furthermore, the resistivity of the resistive unit could be determined, a task previously not possible with surface geophysical methods.
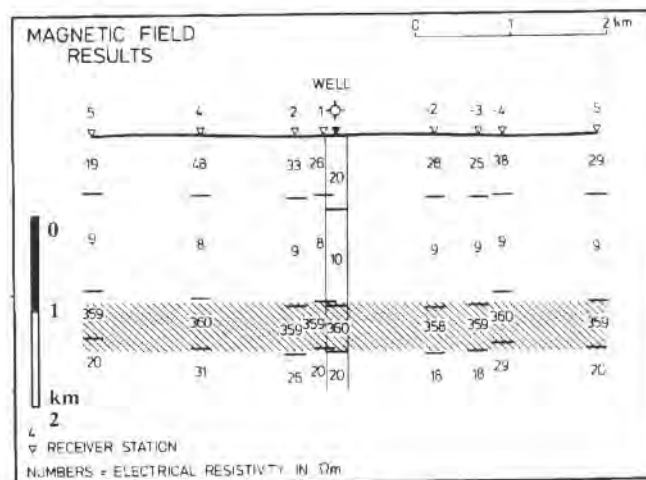

Fig. 8.4: Inversion results based on the magnetic response data using both transmitters. The depth to the top of the resistive region (shaded) is resolved but not its resistivity or thickness (after Strack et al, 1989b).
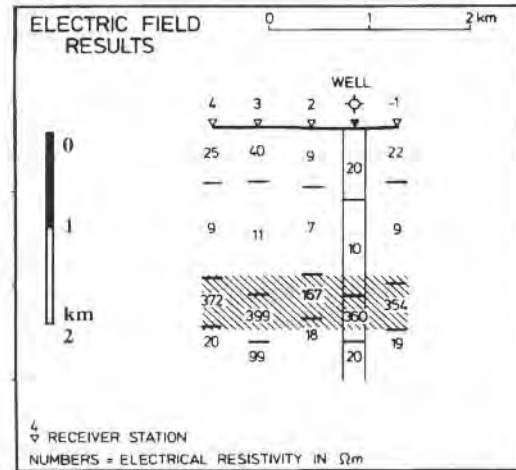
Chapter 8

Fig. 8.5: Inversion results based on the electric field data using both transmitters. The depth to the top of the resistive region (shaded) is resolved, as is its resistivity (after Strack et al, 1989b).
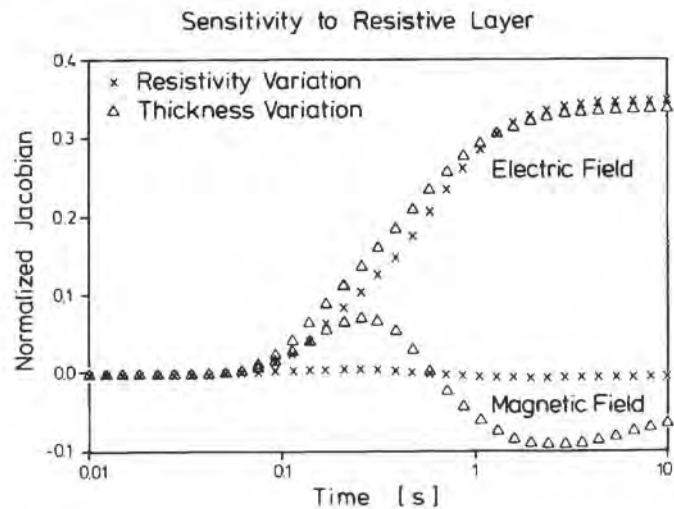

Fig. 8.6: Resolution analysis for the resistive layer parameters using the normalized Jacobian as a measure of sensitivity. The magnetic field (bottom two curves) is almost insensitive to changes in the target layer resistivity, whereas the electric field (top two curves) is very sensitive to both thickness and resistivity variations (after Strack et al, 1989b).

CANNING BASIN, AUSTRALIA, CASE HISTORY

In evaluating LOTEM in Australia, the capabilities of the method for resolving variations in resistive strata was of particular interest in the Canning Basin (figure 8.7). Minor production is obtained from porous zones within the very extensive Windjana / Nullara limestone of Devonian–Famenian age (figure 8.8). The limestone is easily mapped by reflection seismic surveys, as is shown below. The major exploration difficulty has been in locating zones of adequate porosity.
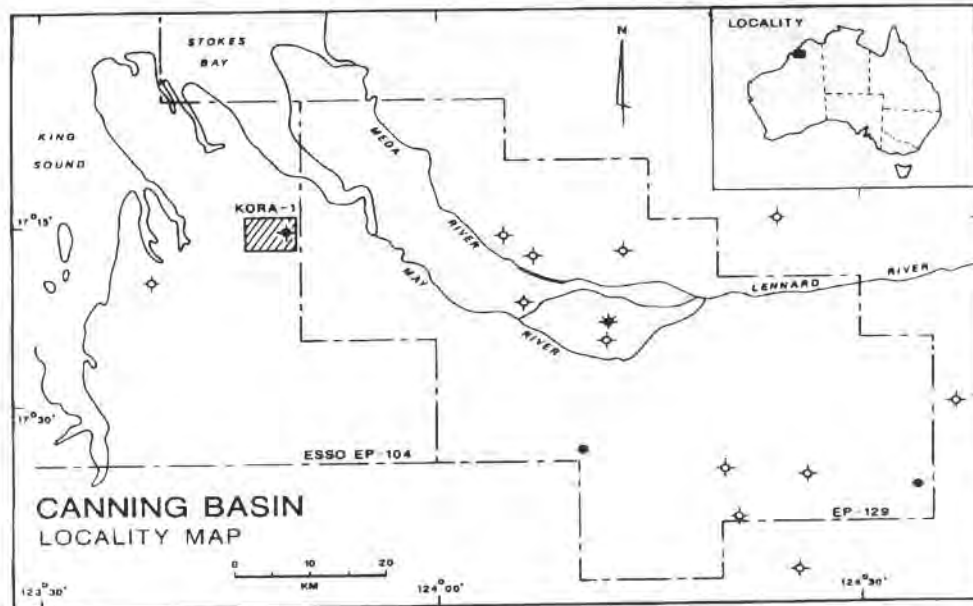

Fig. 8.7: Basemap of the Australian survey (after Strack et al, 1989b).

For evaluation purposes a region was selected where high quality seismic sections and good well logs were available. Kora–1 (figures 8.7 – 8.13, 8.15) had already been completed and West Kora (figure 8.9) was being drilled in mid–1985 when the LOTEM survey was undertaken. Both holes showed poor porosity. A geological section through Kora–1 is shown in figure 8.8. As the well bottomed in the Napier formation, lithology and structure below drilling depth are conjectural.

Figure 8.9 shows the LOTEM survey plan. LOTEM measurements were conducted using a current of 30 Amperes through approximately 1.5 km long grounded wire dipoles. Both electric and magnetic field measurements were made on line 4 from transmitter 2. The area was electrically relatively quiet, which resulted in clean field data.
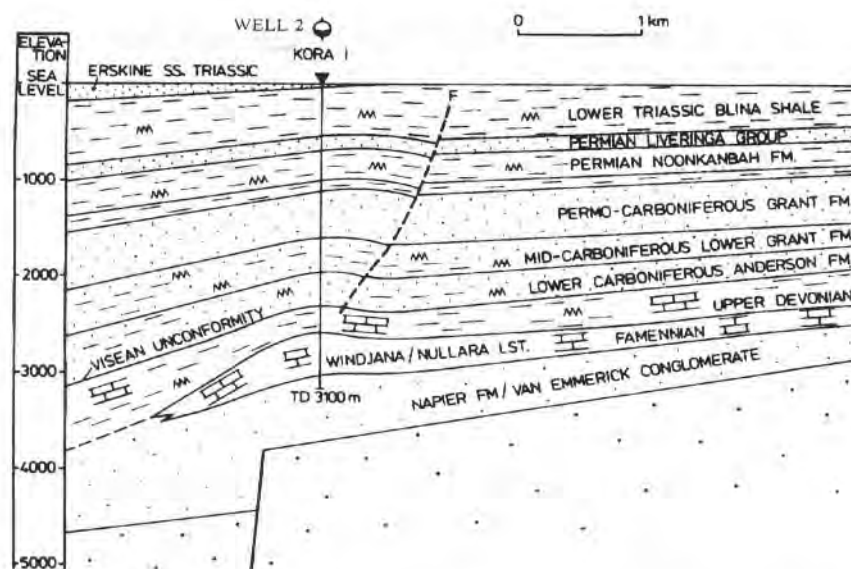
Fig. 8.8: Geological cross section for the Canning Basin LOTEM survey area (after Strack et al, 1989b).
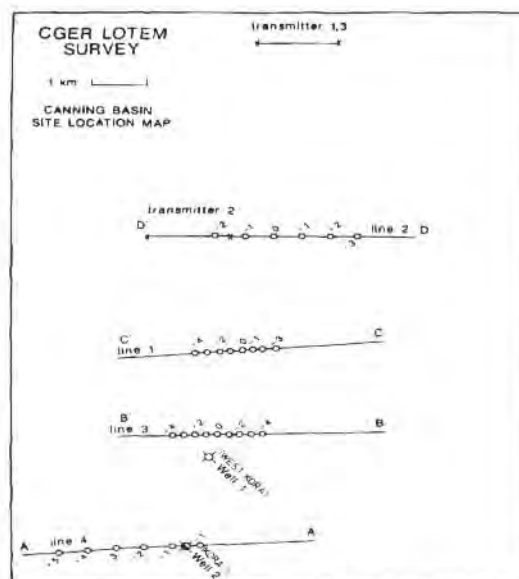

Fig. 8.9: Canning Basin LOTEM survey plan (after Strack et al. 1989b).

Assuming that the seismic data accurately represented depth variations along the line, LOTEM data were inverted starting at the well Kora–1 (figure 8.10) to investigate resistivity variations within the various units. The good quality of the seismic results shown figure 8.11 and the blocked well log from figure 8.10 motivated the use of a 9
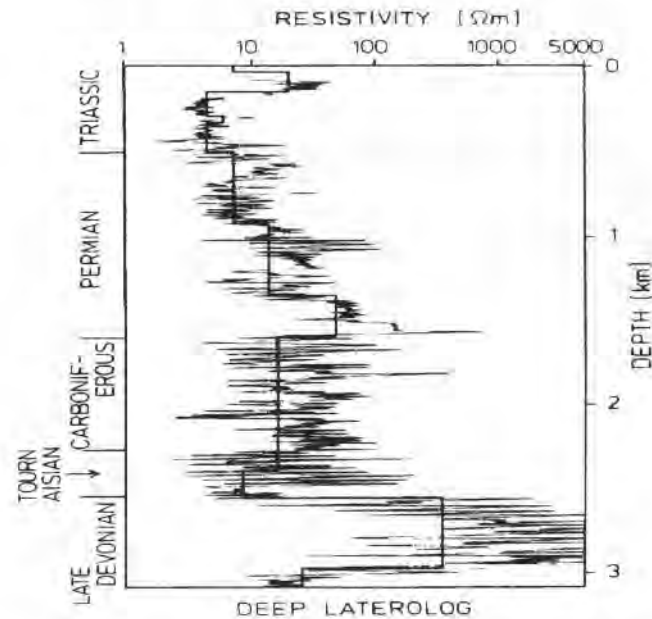

Fig. 8.10: Well log with blocked model (heavy line) for the well Kora–1 in figure 8.9 (after Strack et al, 1989b).
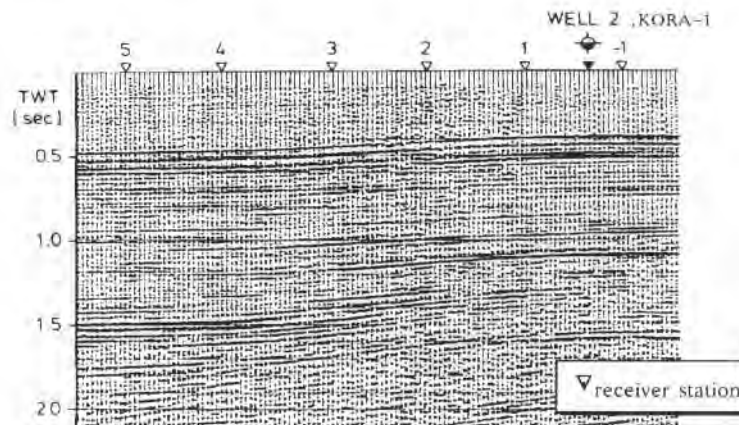

Fig. 8.11: Seismic section for line 4 which was used to fix the geologic structure for the inversion (after Strack et al, 1989b).

or 10 layer model, which would have otherwise been unthinkable. The layer thicknesses were kept fixed in inversion on the basis of seismic mapping. Figure 8.12 shows interpreted resistivity variations based on the magnetic component data only. The values shown for the resistive carbonate (unit i) were poorly resolved by the inversion when only magnetic data were used. However, when the electric field data were added for joint inversion, the results shown in figure 8.13 were obtained. Now the resistivities of the carbonates are much better resolved.
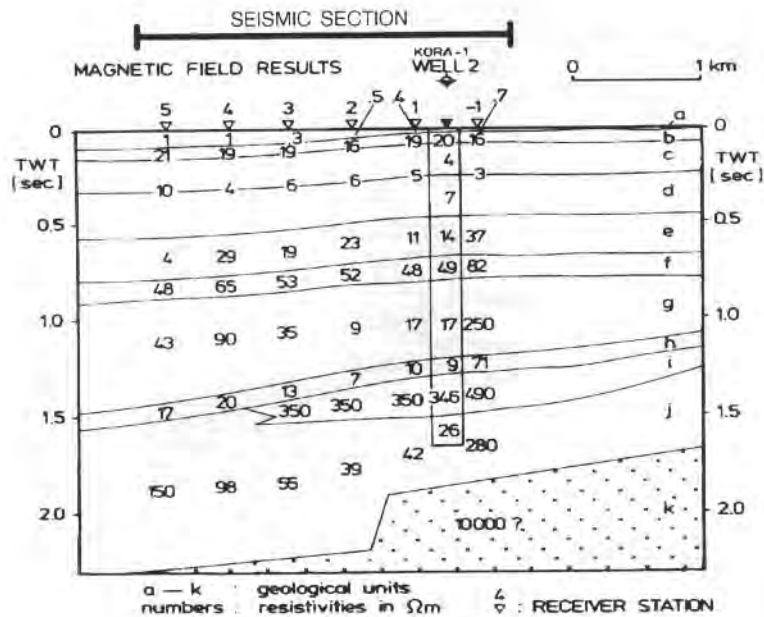

Fig. 8.12: Resistivity variations within units, obtained from magnetic transient data by fixing all layer thicknesses according to seismic information and inverting for the best fitting resistivity values. Confidence in Unit i values is poor because it is resistive (after Strack et al, 1989b).

Under the assumption that, within each unit, water resistivity and water saturation were constant, the expected variation of resistivity with sand–to–shale ratio for each clastic unit (Schlumberger, 1987, chapter 2) was calculated. Figure 8.14 shows the relationship for unit e. Using similar calibration curves for each unit allowed us to transform resistivity variations to percent sandstone within clastic units. For the carbonates, unit i, it could be assumed that Archie's formula (Archie, 1942) relates resistivity variations to porosity variations (Schlumberger, 1987). Figure 8.15 shows the results of transforming the resistivity section of figure 8.13 to percent sandstone ratios. The variations within unit i are seen to be small, indicating a uniformly low porosity.
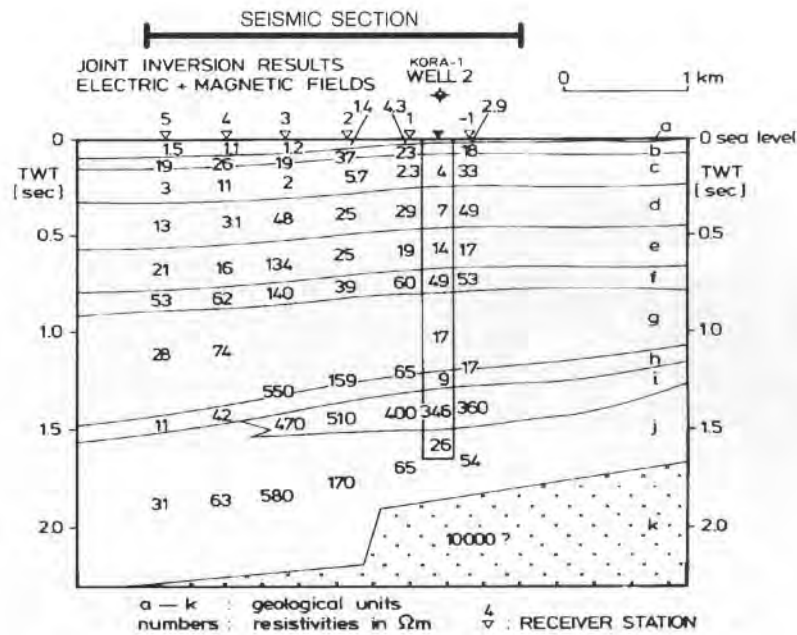
Fig. 8.13: Resistivity variations within units. They were obtained from magnetic and electric transient data by fixing all layer thicknesses according to seismic information and inverting for the best fitting resistivity values using joint inversion. The statistical confidence in the resistive unit i is much greater than in figure 8.12 (after Strack et al. 1989b).
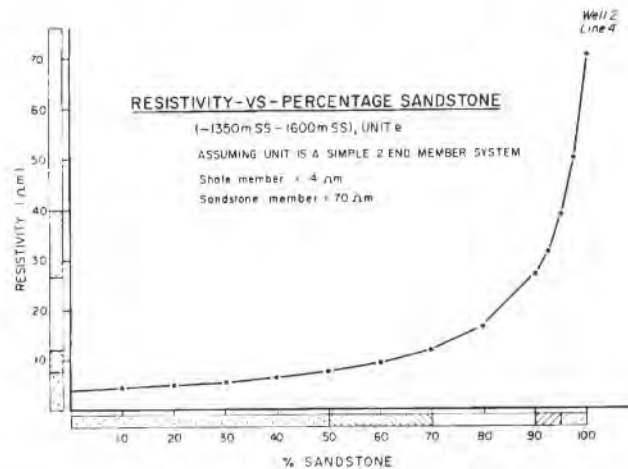

Fig.8.14: Resistivity versus percentage sandstone for unit e. The relationship is derived from the well log and used to convert the interpreted resistivity values to sand-to-shale ratios (after Strack et al. 1989b).
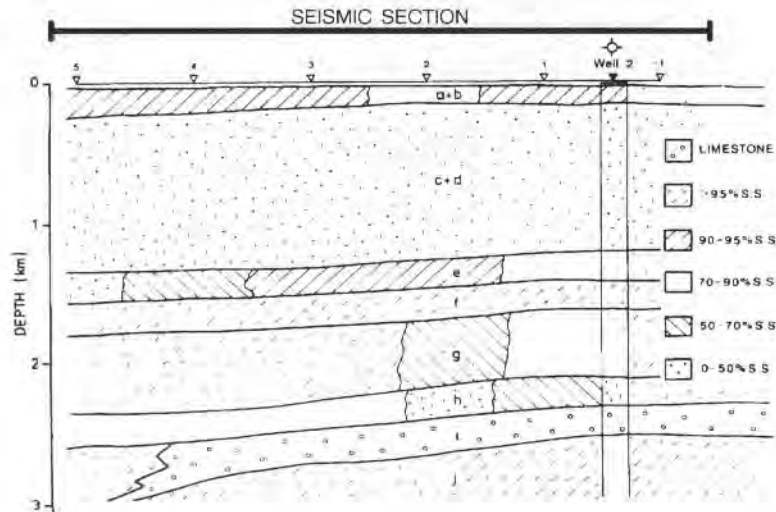
Fig.8.15: Resistivity section in terms of sand–to–shale ratios, reflecting porosities under the assumption that salinity and water saturation do not vary laterally same within a clastic unit. The percentage sandstone values were derived using the calibration curve and the scales along the axis from figure 8.14 (after Strack et al, 1989b).

This example demonstrated the benefits of jointly inverting electric and magnetic transients as well as the successful use of seismic data to achieve higher resolution in the EM data. It also shows that with high quality data and integrated interpretation, a porosity map of the subsurface can be obtained.

TAI XING AREA, PRC, CASE HISTORY

During 1988, a LOTEM survey was carried out in China within the German TEM Pilot–Demonstration Project. The survey area is located in the Jiangsu province which is tectonically located at the junction of the Yangtze and Huabei paraplatforms. Many oil and gas shows are found in the area. From the Cambrian to the Triassic, the area underwent orogenic and transgressional-regressional cycles. The sediments have a total thickness of between 3000 m and 9000 m. In parts of the area, the sediments include carbonates and/or volcanic material within the section. Both can give significant problems with reflection seismic data. The objective of the LOTEM demonstration survey was to define the structure of the carbonates/volcanics and possibly to investigate the strata below it. Very little additional geological information was available before the survey was carried out. The geophysical information consisted of a seismic section, one interpretation map (top of Triassic) and a well log. Although the seismic data shown in figure 8.18 are not very good, they clearly show

three reflectors as marked in the figure. On the left side of the section, the data quality become poor and one would expect a structured depression.

Seismic Section 3220

Well 174

TWT

Quaternary

Cretaceous

Triassic

0

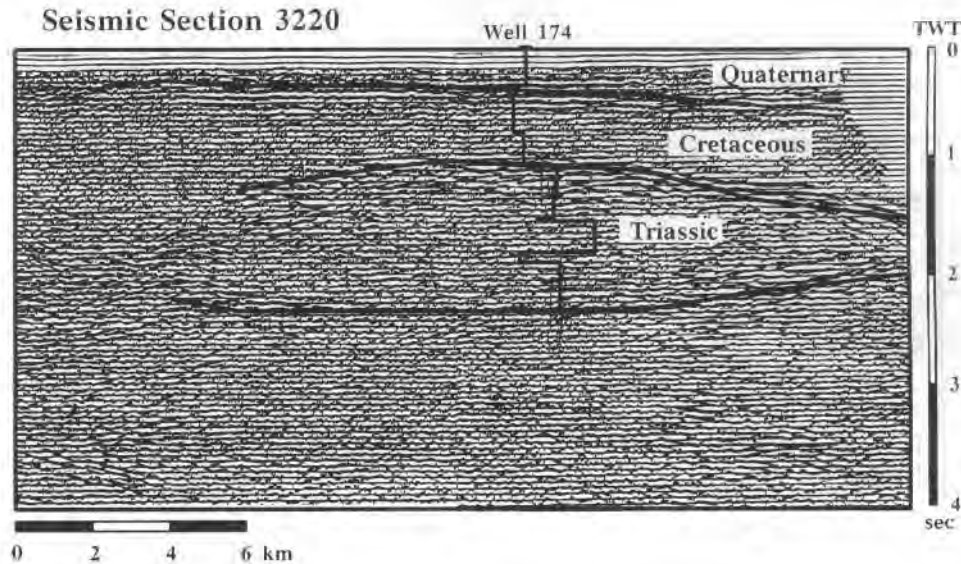1

2

3

4
sec

0   2   4   6 km

Fig. 8.18: Seismic section for line 3220 with three interpreted reflectors.

From this section and other (not available) data a contour map showing the top of Triassic was derived and is given in figure 8.19. The objective was to map the top of the Triassic, Permian and Carboniferous carbonates and possibly structures within and below the carbonates. The overall goal of the project was to demonstrate the LOTEM technique in this environment in comparison with other methods. From the geology and the seismic section the lowest reflector in figure 8.16 is thought to be the top of Devonian.

The LOTEM survey was designed to measure one profile as close as possible to seismic line 3220, the coordinates of which are not exactly known. The survey plan and the approximate location of the seismic lines are shown in figure 8.18. In addition to the profile parallel to the seismic line, a walkaway test from the transmitter was carried out. This was done because only one transmitter was used in the survey area and the effect of possible transmitter overprints had to be checked. Also displayed in figure are the power lines in the survey area. The density of the power lines and the variable power line frequency might make magnetotelluric measurements very difficult. It appears that only a controlled source technique could overcome this problem.
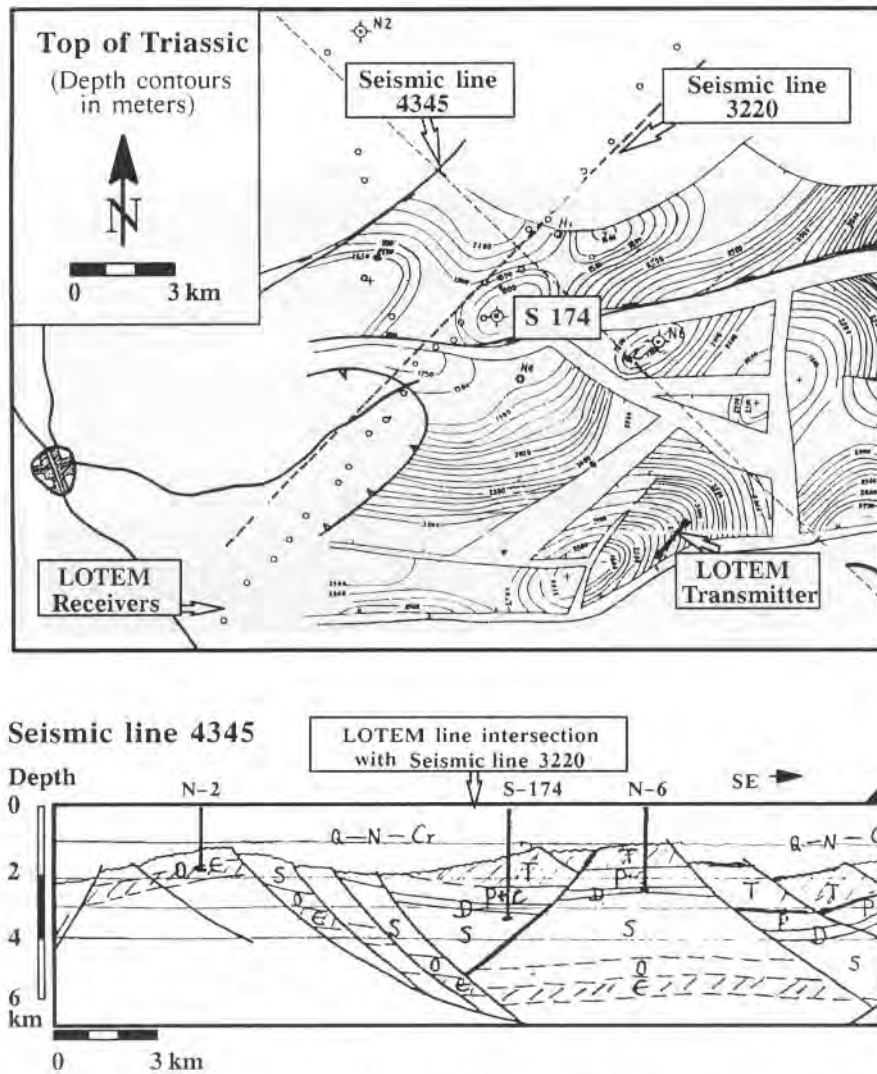
Fig. 8.17: Contour map derived from seismic information of the top of the Triassic. The south-
western part of the seismic line 3220 shows a depression. At the bottom a geological
section along a perpendicular seismic line in shown.

From the well log information different, blocked logs were derived and are shown
in figure 8.19. The solid line represents a well log which was blocked based on the
lithology only. Significant features in this log are the rise in resistivity for the Triassic
and Permian limestones. The dashed line in the figure represents a blocked well log
after forward modeling for the LOTEM method. Now, only three layers can be

distinguished. One layer boundaries just below the Cretaceous siltstones and the others is at the top of the Triassic limestone. The Permian limestone could not be distinguished according to forward modeling.
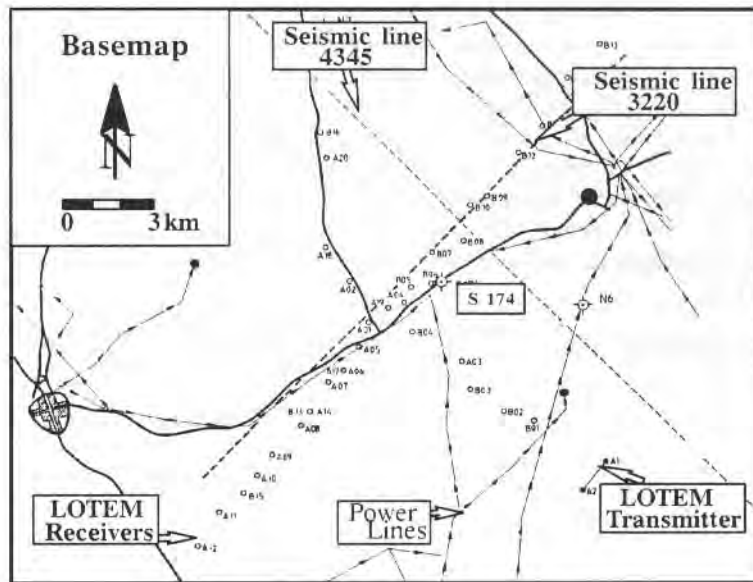

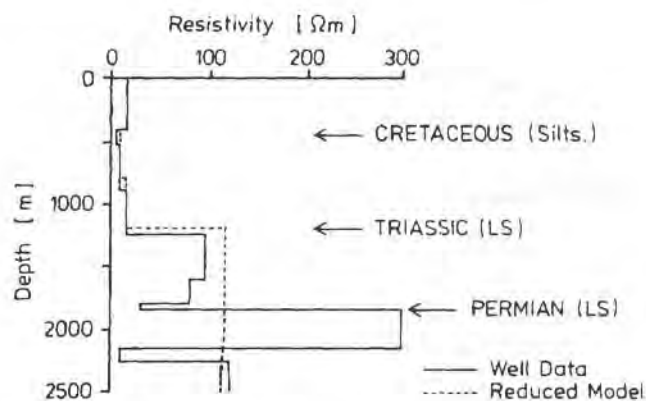Fig. 8.18: Survey plan of the LOTEM survey near Tai Xing, PRC.

Fig. 8.19: Two reduced induction logs. The blocked one represents the blocked preserving the lithology and the dashed one considers LOTEM layer resolution.

The results from the forward modeling caused by the parameter variations for the electric and magnetic field components are shown in figure 8.20. Here, the resistivity

of the Permian carbonates was varied. The changes simulate variations in porosity in the limestone. The magnetic field derivative is displayed as early and late time apparent resistivity curves, while the electric field is displayed as voltage measured at the receiver. The magnetic field response shows variations from 0.1 seconds to 10 seconds. The variations span in amplitude range of about 2.5 decades. The electric field shows variation within the same time window but only over about 0.5 decade of amplitude. Also, the differences in the electric field are larger than with the magnetic field response. For both, the magnetic and electric field response, the variations are small and, if detectable, the electric field stands a better chance of succeeding. From this type of forward modeling curves, it was concluded that the LOTEM survey had only a limited chances of succeeding in the discrimination of structures within the carbonates. It could detect the top of the combined Triassic, Permian and Carboniferous carbonate unit and its average resistivity, but not detail within and below this unit.
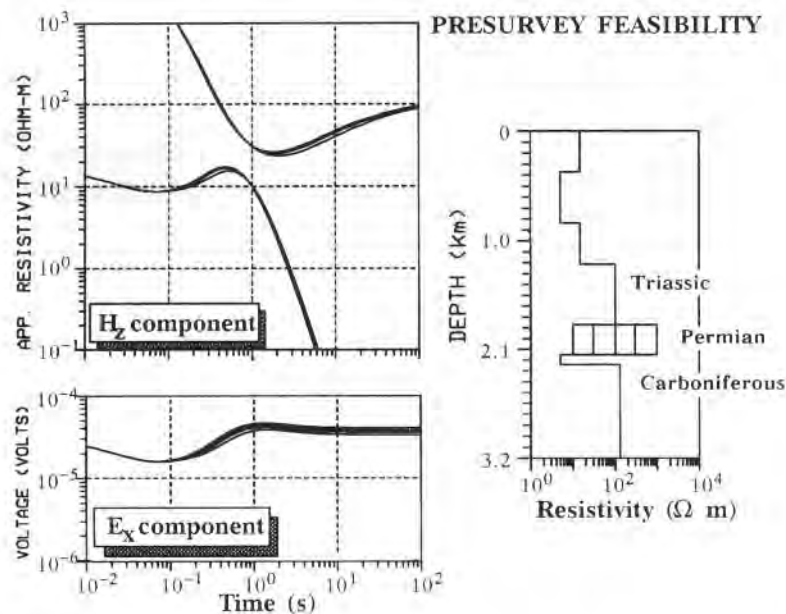

Fig. 8.20: Synthetic LOTEM curves for the magnetic and electric field responses for porosity (thus resistivity) variations in the Permian limestone.

The field data were processed in the field using standard procedures as described in previous chapters. The data were then interpreted using a one-dimensional layered earth inversion program. The results were plotted as a resistivity section and are displayed in figure 8.21. On top of the inversions two of the three seismic reflectors are superimposed. For the depth conversions an average velocity of 2.5 km/s was used (more detailed velocities were not available). The match between the seismic

reflectors and the layered inversion results in figure 8.21 is remarkable. To judge the reliability of this fit we must consider the following:

○ The field data were processed in the field which means that no fine tuning of the processing for the optimum signal–to–noise ratio was done.

○ The depth conversion of the low quality seismic data was done using only an average seismic velocity because detailed stacking velocities were not available.

○ The presurvey forward modeling suggests that we can only resolve the top of the carbonates average resistivity.

○ Detailed statistical and resolution analysis of the inversion results was not done.
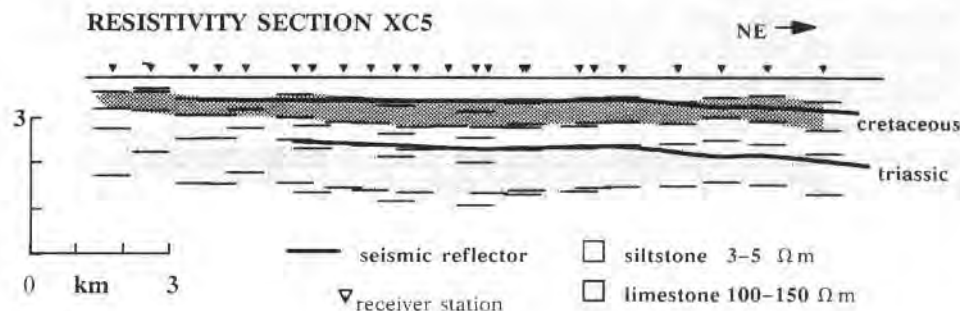
RESISTIVITY SECTION XC5

Fig. 8.21: Resistivity section derived from one–dimensional inversions for the LOTEM profile. Superimposed are the seismic reflectors.

In light of the above factors, one would not trust the the results displayed in figure 8.21. When inspecting the inversion statistics, it becomes clear that none of the parameters (layer resistivities and thicknesses) below the Triassic limestone top are resolved. The inversion simply maintained the starting model which was derived from the well log. This presents a serious problem with these data, because it means that the layered earth model assumption had reached its limits. Thus the field data were reinspected and other ways of displaying data were considered. In this case we used the source or current imaging technique described in chapter 2 was used. Figure A.7.8 (appendix 7) displays the result of the current imaging with the seismic section superimposed to it. One can clearly see the depression in the LOTEM current image which is consistent with the depression in the seismic data. Further, the top of the carbonates is clearly visible as start of the resistive unit. There are also variations visible in the blue image which represents data within the carbonates. However, to confirm that these variations are real one would need additional information such as well logs and/or better seismic data.

The case history near Tai Xing clearly shows that the LOTEM technique has a higher potential than we are hereto able to interpret. When considering that the LOTEM image section is constructed with about 30 records while the seismic section uses several thousand traces, the interpretation results are very good.

SUMMARY CHAPTER 8

Most surface controlled source (inductive) and natural source electromagnetic methods are strongly biased towards the more conductive parts of the geoelectric section. The case histories show that LOTEM can be successfully applied in exploration of hydrocarbon reservoirs where the task is to define variations in the resistive part of the geoelectric section. In examples from Europe and Australia LOTEM provided specific information for the section with an accuracy previously not possible. An increased use of LOTEM with both electric and magnetic field measurements will yield more experience with the method. Only the gain in experience will conclusively show whether or not the technique can be adopted as a routine tool to oil exploration.

In the first case history, only the electric field measurements showed sensitivity for the resistive parts of the section. In the case history from the Canning Basin, joint inversion of LOTEM electric and magnetic fields provided a way to derive a porosity map of the subsurface.

The last case history from China illustrates the limits of one–dimensional inversion. The inversion results were unreliable although they match with the information available from seismic. A different technique using directly the field data had to be used. The current or source imaging technique proved to be the most reliable one. In addition to confirming the *a priori* information trends can already be recognized in the source imaging. This indicates that the LOTEM method has a higher resolving capability as hereto used.

PROBLEMS CHAPTER 8

1. What is the difference between the use of the magnetic field and the electric field components?
2. How do you confirm that one–dimensional interpretation is applicable and gives valid results?
3. How can you see from figure 8.4 that the inversion do not resolve the resistivity of the third layer?
4. How was the sand–to–shale ratio map (figure 8.15) derived for unit i?
5. Which electromagnetic techniques do you consider applicable in the Tai Xing area? Please elaborate.
6. How can you see that the interpretation in figure 8.21 is unreliable?

KMS Technologies – KJT Enterprises Inc.
6420 Richmond Ave., Suite 610
Houston, Texas, 77057, USA
Tel: 713.532.8144

Please visit us
http://www.kmstechnologies.com